# Chapter 5

NUMERICAL RESULTS AND DISCUSSION

Both steady-state system throughput and average packet delay are evaluated for both correlation and chip-level receivers, taking into account the effect of MAI, shot noise, and thermal noise. The results are divided into three sections, the first and second sections show the system performance with MAI only for both two- and general-class networks, respectively. The third section presents the performance of the network in presence of MAI with shot and thermal noises, separately, in a network of general number of classes. Our results are evaluated for a network of 30 users and a 2D OCFHC/OOC code with $p = 2$, $k = 2$, $N_{OOC} = 7$, and $w = 3$. That is the cardinality is 12 codes (Eq. (4.1)).

Fig. 5.1 shows that using OCFHC/OOC is the best choice not only is it increasing the cardinality but also OCFHC/OOC slightly improves the network performance than OOC for Pro 1 and Pro 2 as shown in Figs. 5.1(a), 5.1(b), respectively.

5.1   TWO CLASSES NETWORK

The available 30 users are divided into two classes. Assume that $N_1 = 10$ users are in Class 1 and $N_2 = 20$ users are in Class 2. The available codes are distributed equally between the two classes $\mathcal{C}_1 = \mathcal{C}_2 = 6$.

The total throughput of the network versus the user activity for the two different protocols (Pro 1 and Pro 2) are plotted in Figs. 5.2 and 5.3 for both correlation and chip-level receivers. In Fig. 5.2, we assume that the number of codes per Class-1 user equals 2, while in Fig. 5.3, we assume that the number of codes per Class-1 user equals 6. For Pro 1, the throughput reaches a saturation level because the available codes are less than the total number of users. That is, when all available codes are assigned, any new active user has to wait until a code is released. While for Pro 2 the total throughput increases
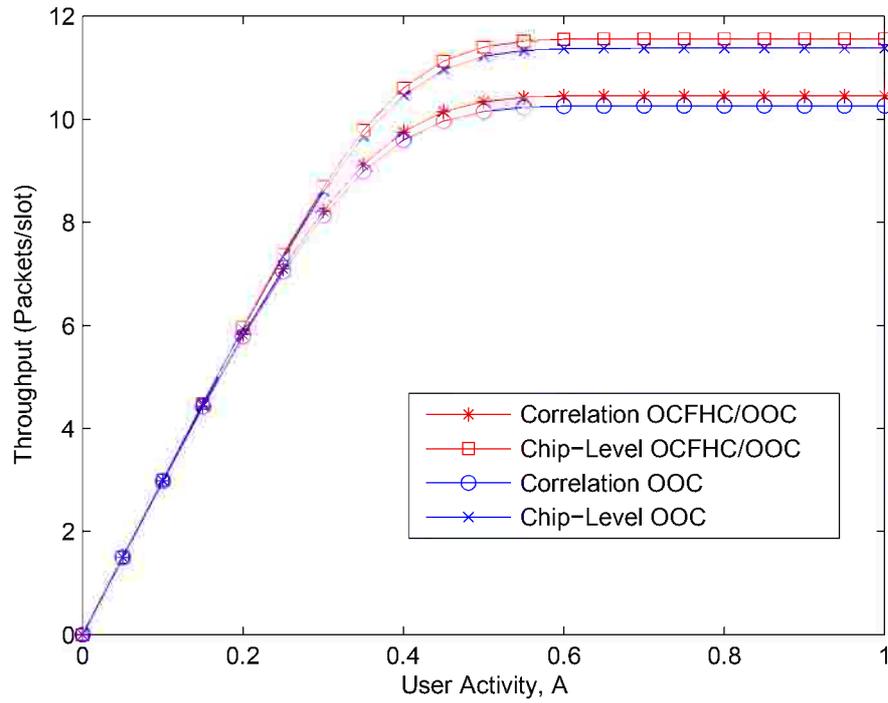
(a) For Pro 1.
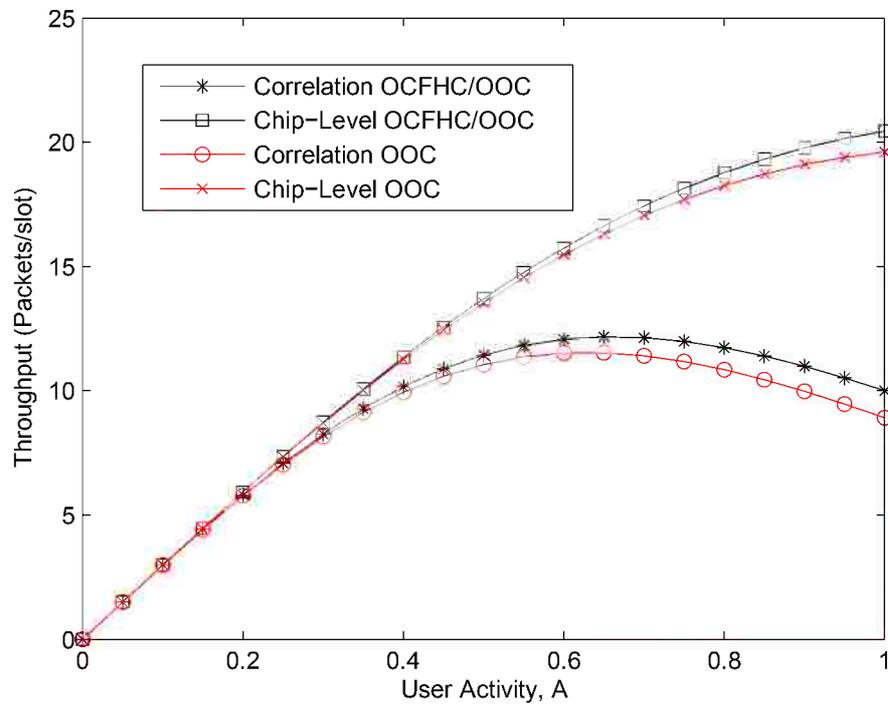
(b) For Pro 2.

FIGURE 5.1 Total throughput vs user activity for Single-rate Class Network using OOC and OCFHC/OOC
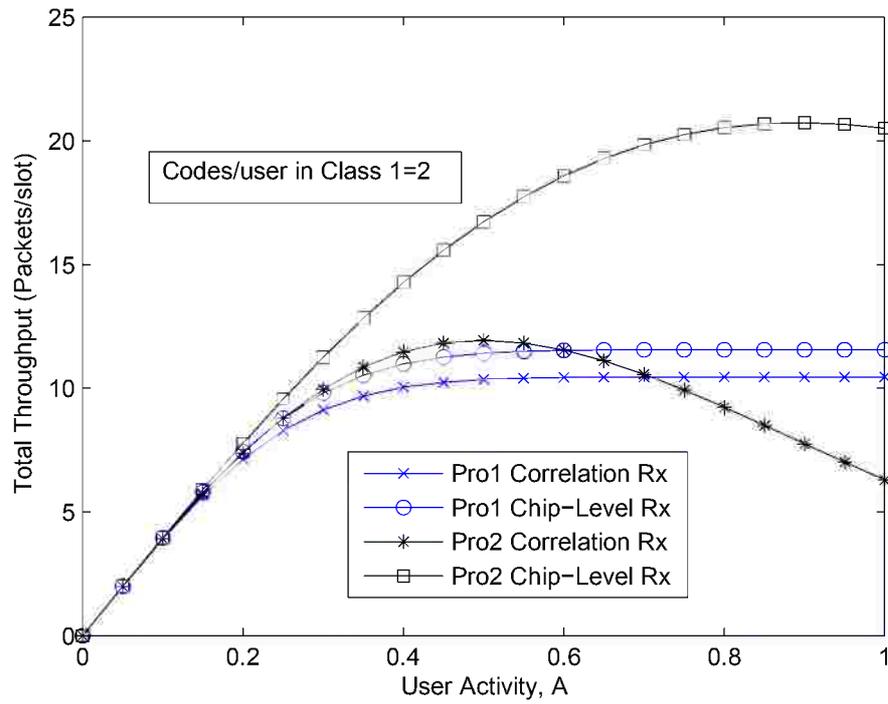
FIGURE 5.2 Overall network throughput versus user activity for number of codes per user in Class 1 equal 2.
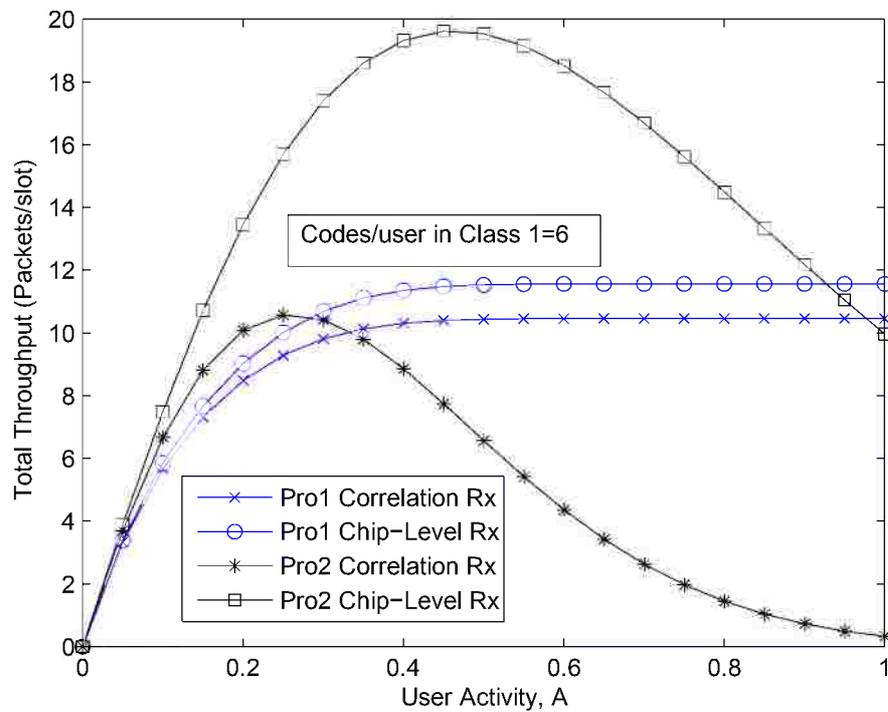

FIGURE 5.3 Overall network throughput versus user activity for number of codes per user in Class 1 equal 6.

until it reaches a maximum value and then decreases with increasing the user activity (due to the increase of interference probability). It can also be seen that, when using a correlation receiver, the total throughput of the two protocols are close to each other at small values of user activity; these values depend on number of codes per user in high rate class. It appears that Pro 1 is appropriate for correlation receivers. On the other hand, when using chip-level receiver, the total throughput of Pro 2 is much better than Pro 1 for almost all activities. Moreover, the rate of the decay of the total throughput for Pro 2 as the activity of the users increases for chip-level receiver is slower than its correspondent for correlation receiver due to the powerful capability of chip-level receivers in attacking multiple-access interference. One final remark for Pro 2 is that as the number of codes per a Class-1 user increases, the throughput would decay faster after reaching its peak value. Indeed from Fig. 5.3, an active user is assigned 6 codes (probably used) to transmit its data, which dramatically increases the interference and packet drops more frequently.
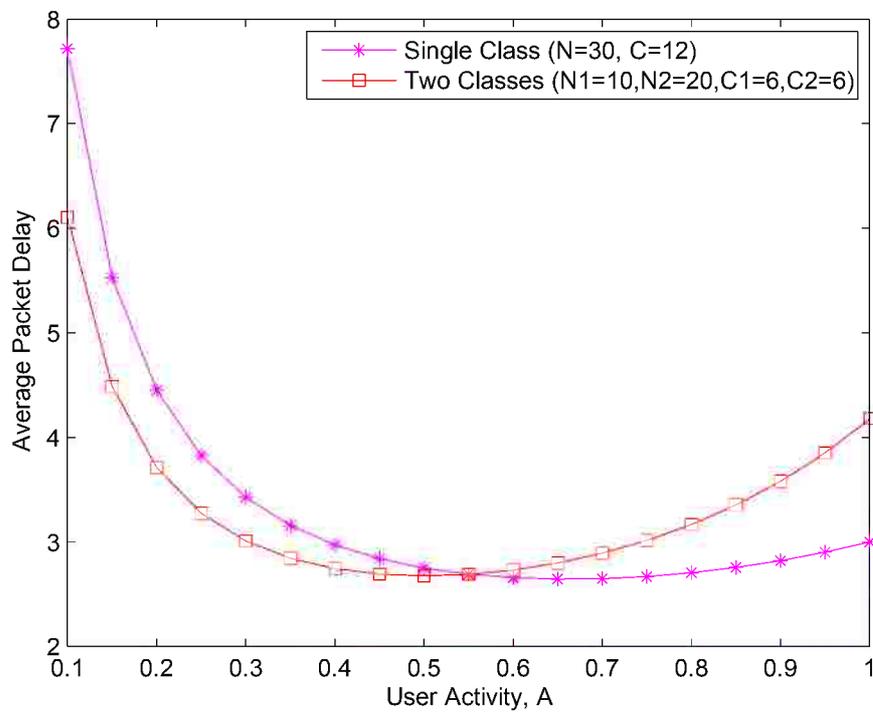
The average packet delay of the correlation-receiver network is plotted in Fig. 5.4 versus the user activity for the two protocols. For the sake of comparison, the results of the single-class network is also plotted in the same figure. We can note that at low user activity the average packet delay of the two-class network is very close to that of the singe-class network in the case of pro 1. However, the average delay of the two-class network is smaller in the case of pro 2. On the other hand, at high user activity, the average delay is slightly higher in the case of two-class network for both protocols where at user activity $A = 1$, D is approximately 0.5 time slot.

5.2 GENERAL NUMBER OF CLASSES

To generalize our case study, users of many rates are allowed to access the network. They are divided into several classes, each operating at a different rate (different values of m_x). In our calculations we consider three- and four-class networks and compare the results with that of single rate network [3]. Values of m_x are selected for the three- and four-class networks to be $\{3, 2, 1\}$ and $\{4, 3, 2, 1\}$, respectively. The users are distributed randomly among the classes and consider the large number of users in the low-rate class as usually demanded. The total throughput is plotted in Fig. 5.5 using chip-level receivers and in Fig. 5.6 using correlation receivers. Figs. 5.5(a), 5.6(a) are for Pro 1 and Figs. 5.5(b), 5.6(b) are for Pro 2. It is clear that, using Pro 2 with chip-level receivers make a noticeable improvement in the network performance (Throughput reachs to 21 packets/time slot) for one- and two-class networks rather than using Pro 2 with correlation receivers. However, increasing the number of classes above two would make it beneficial to use pro 1 rather for correlation and chip-level receivers.
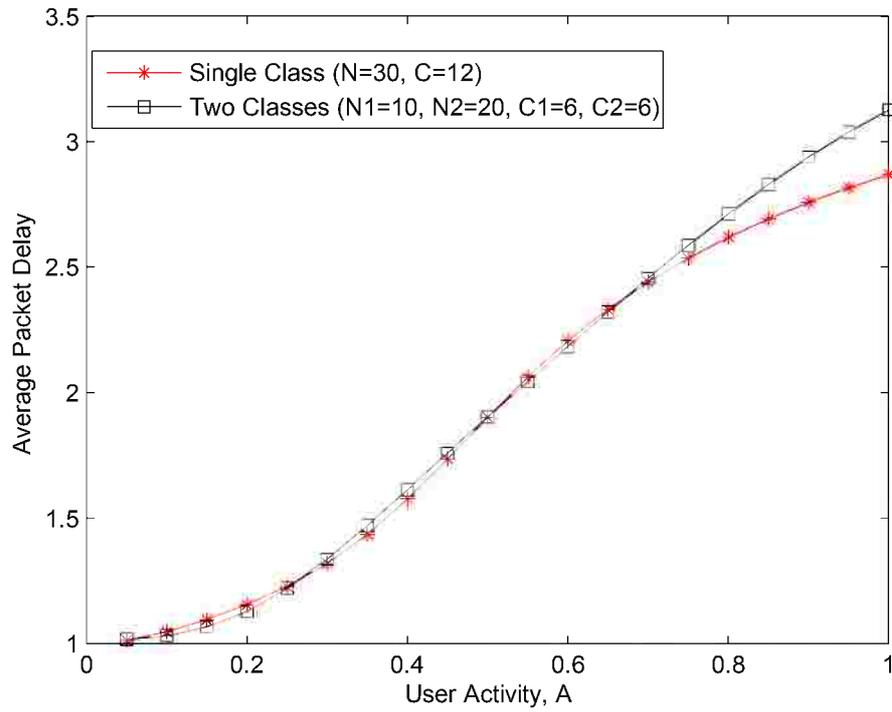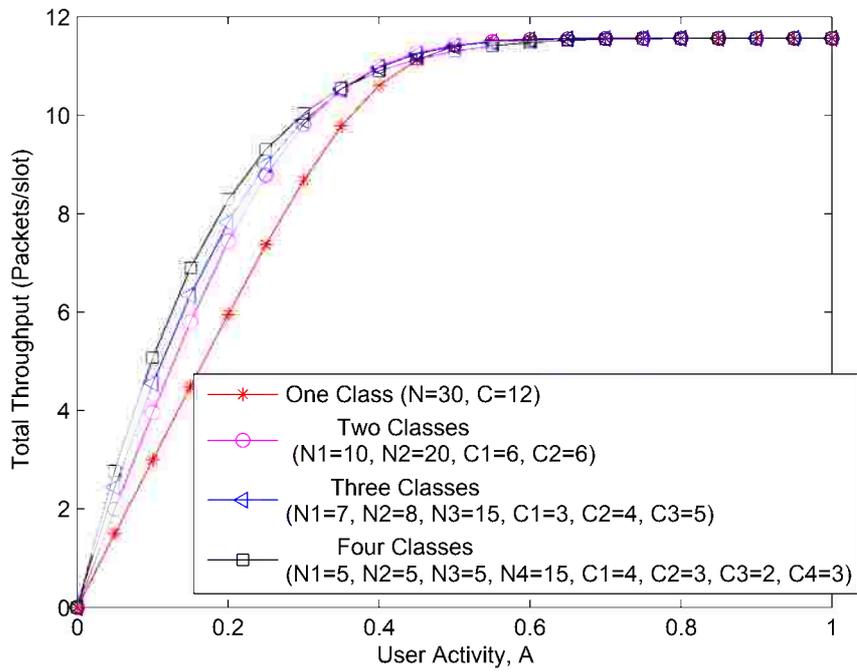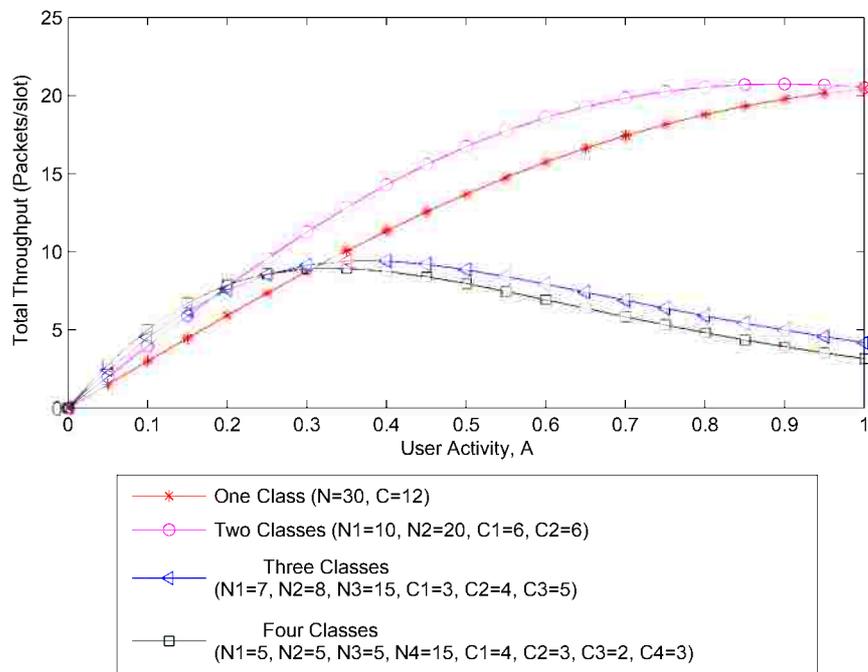
(a) For Pro 1.

(b) For Pro 2.

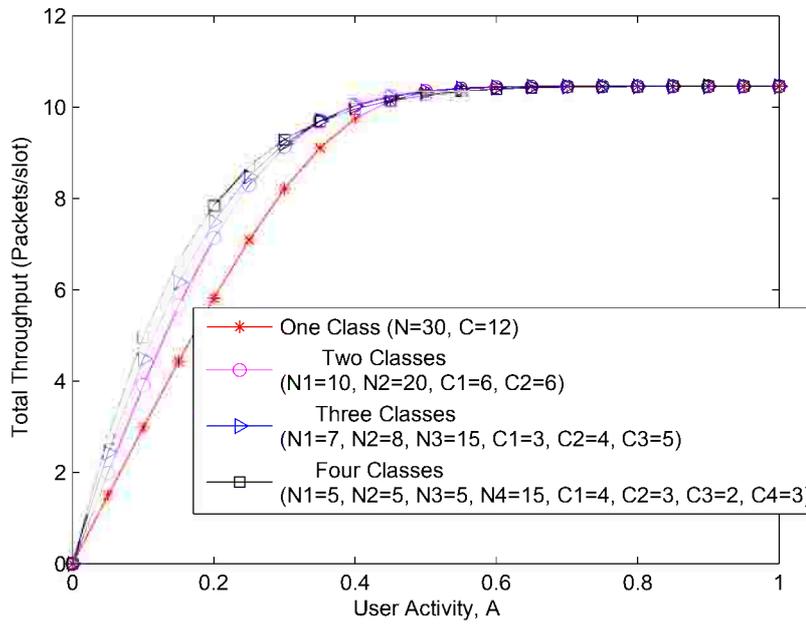FIGURE 5.4 Average packet delay using correlation receiver
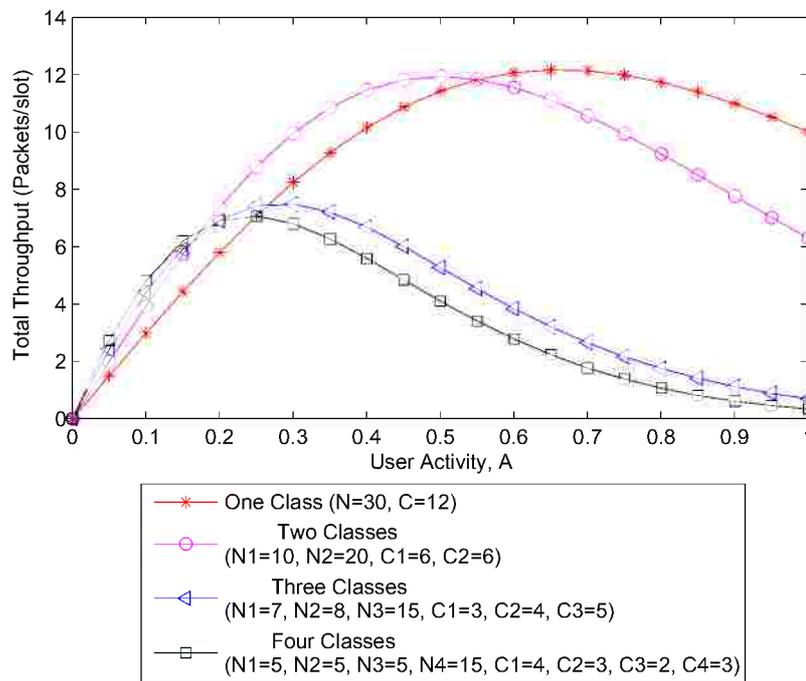
(a) For Pro 1.

(b) For Pro 2.

FIGURE 5.5 Total throughput vs user activity for chip-level receiver (General Classes Networks).
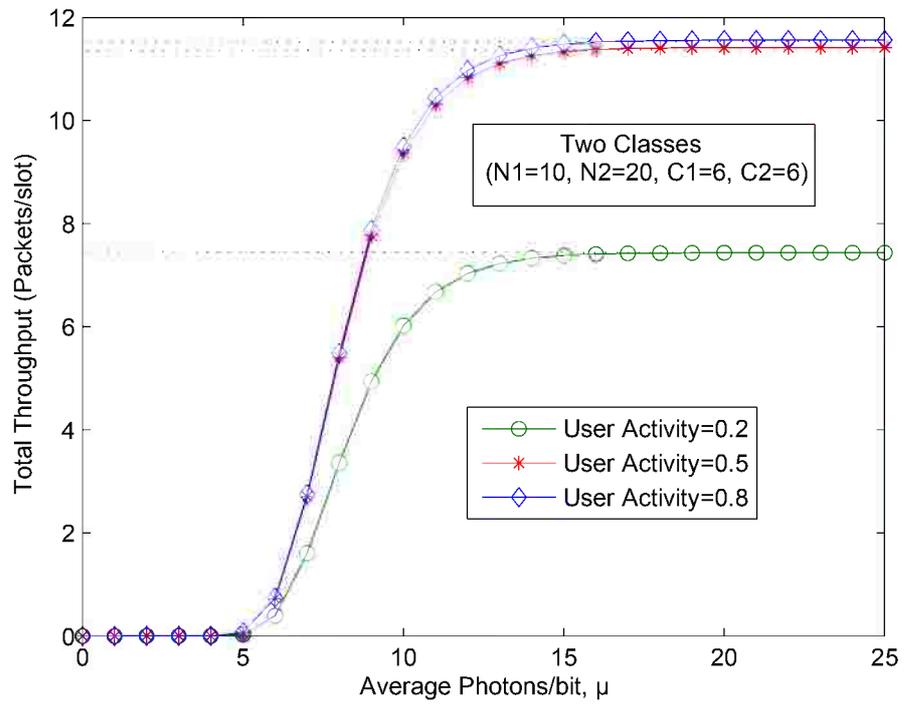
(a) For Pro 1.

(b) For Pro 2.

FIGURE 5.6 Total throughput vs user activity for correlation receiver (General Classes Networks).

# 5.3 EFFECT OF PHOTODETECTOR'S SHOT AND THERMAL NOISES

In this section we consider the effects of receiver noise on the network performance. First, the effect of the receiver's shot noise is taken into account for the case of chip-level receiver with Pro 1 and Pro 2 as shown in Figs. 5.7(a), 5.7(b), respectively. Several average activities have been studied for a two classes network with rates of the users in Class 1 and Class 2 are 2 ,1, respectively. It is clear that, the effect of shot noise in negligible with respect to MAI for the multi-rate network, same as has been concluded for the single rate network [3]. Truly, the throughput rapidly increases from zero to a maximum value, which is identical to the noiseless case by increasing the average received photons/bit from zero to a very small value approximately 15.

Second, we consider The effect of the thermal noise is taken into account for the case of chip-level receiver with Pro 1 and Pro 2. In our evaluation we take the following parameters. Responsivity $\mathcal{R} = 0.84$ A/W, time slot $T_s = 1$ μs, APD gain $G_{APD} = 100$, receiver temperature $T^\circ = 300^\circ$ K, dark current $I_d = 1$ nA, APD effective ionization ratio $k_{eff} = 0.02$, and load resistance $R_L = 50$ Ω. Optimum thresholds θ are used in our plots of Figs. 5.8 and 5.9. Compared to Fig. 5.5(a), It can be seen that the throughput is significantly reduced due to the effect of thermal noise at $P_{av} = -48$ dBm as shown in Fig. 5.8(a). However, as shown in Fig. 5.8(b), slightly increasing the received power to -44 dBm would compensate the thermal noise effect, as shown in Fig. 5.9 at user activity $A = 0.5$. In Fig. 5.10, the bit-error probability for chip-level receiver at $P_{av} = -46$ dBm is plotted versus the decision threshold. It can be seen that when the average laser power is large enough, the optimum threshold is not unique, and it covers a practically wide range. However, when the average peak laser power is not large, then there is only one unique optimum threshold [36]. Finally, implementation tools had used:

1. **Matlab version:**7.10.0 (R2010a) 32 bit.

2. **Hardware:**

   - **Operating system:** Microsoft Windows 7 Professional.
   - **Speed of Processor:** 2.53 GHz
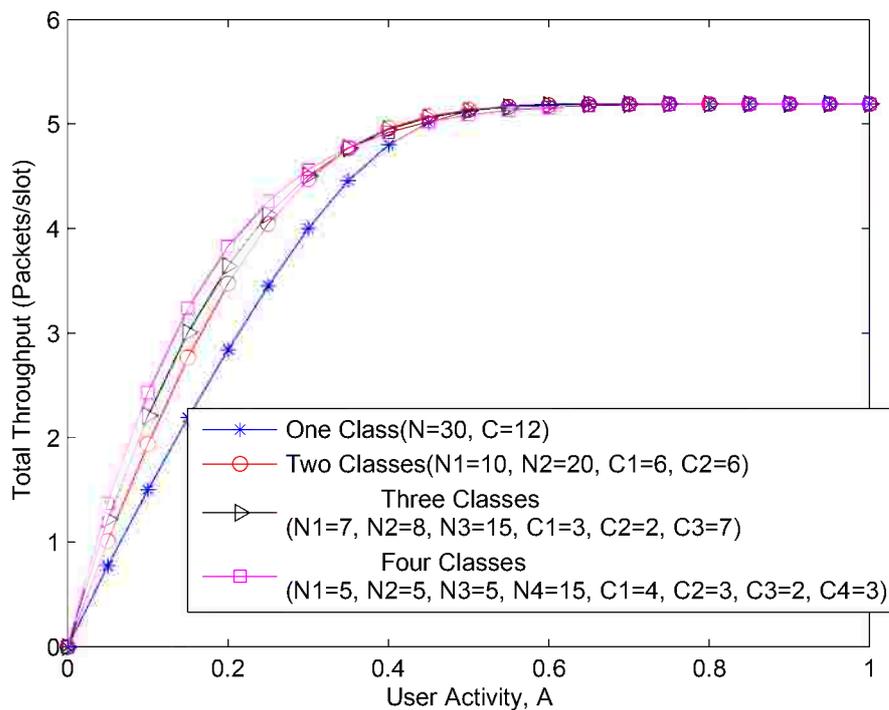   - **RAM:** 64 GB
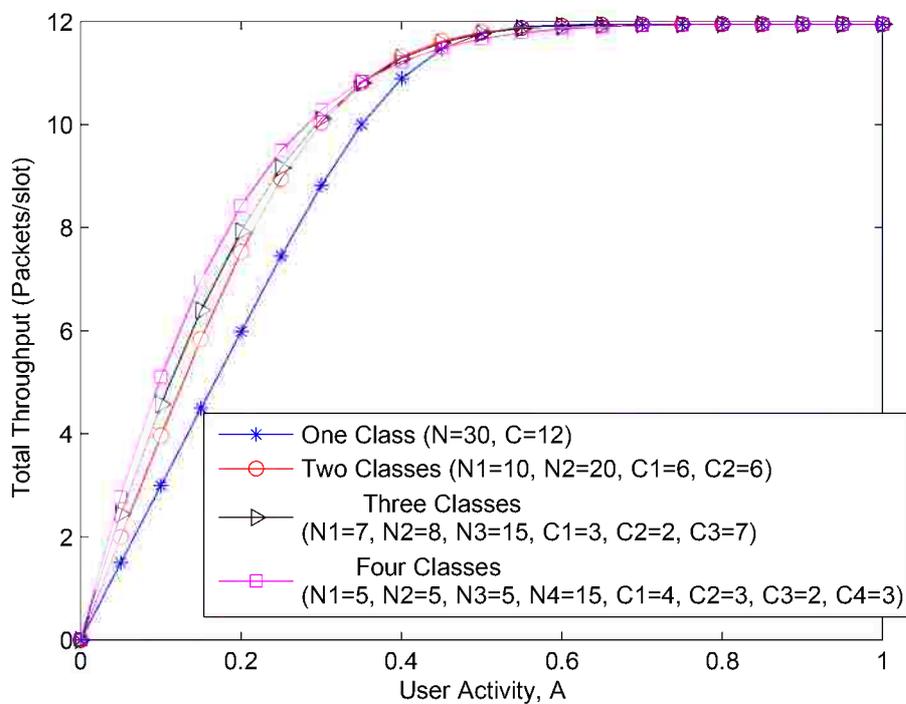   - **Hard disk:** 465.76 GB

(a) For Pro 1.
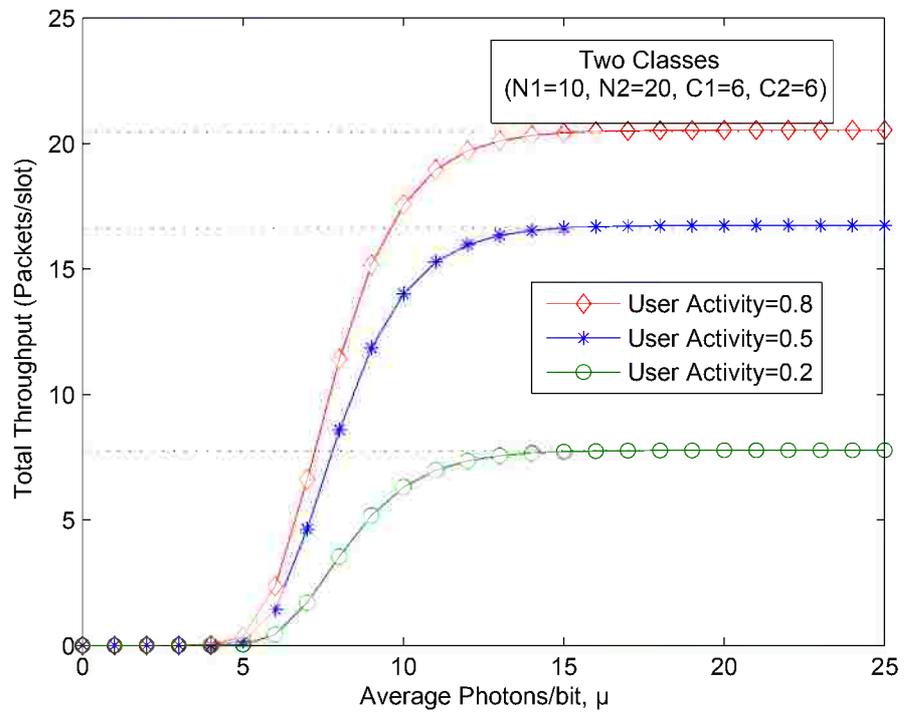
(b) For Pro 2.

FIGURE 5.7 Total throughput vs. average photons/bit for chip-level receiver.

(a) $p_{av} = -48 \quad dBm$

(b) $p_{av} = -44 \quad dBm$

FIGURE 5.8 Total throughput vs. User Activity for chip-level receiver in presence of thermal noise for protocol 1.
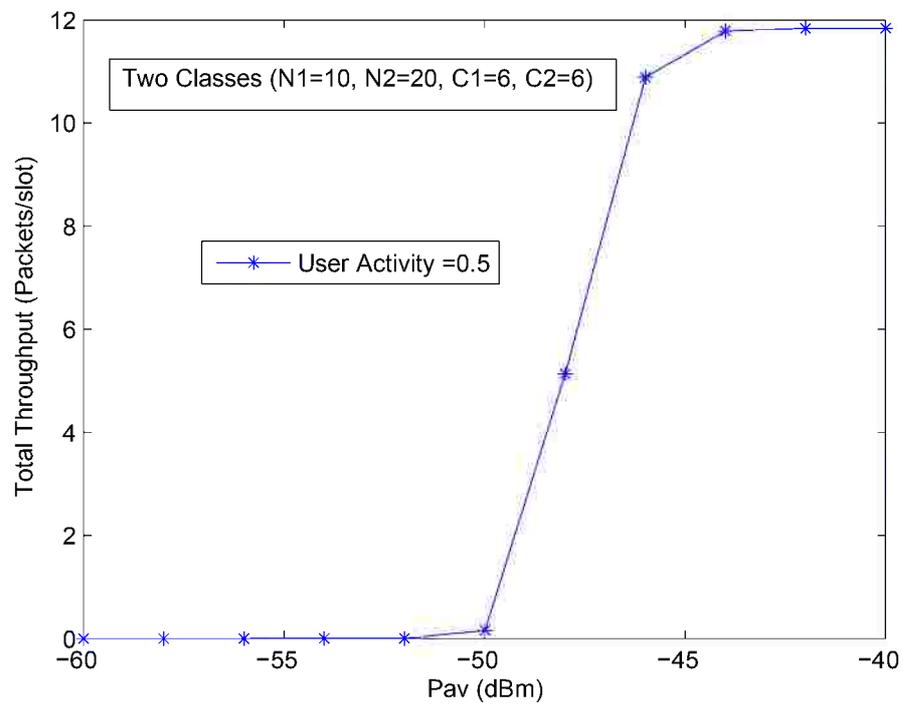
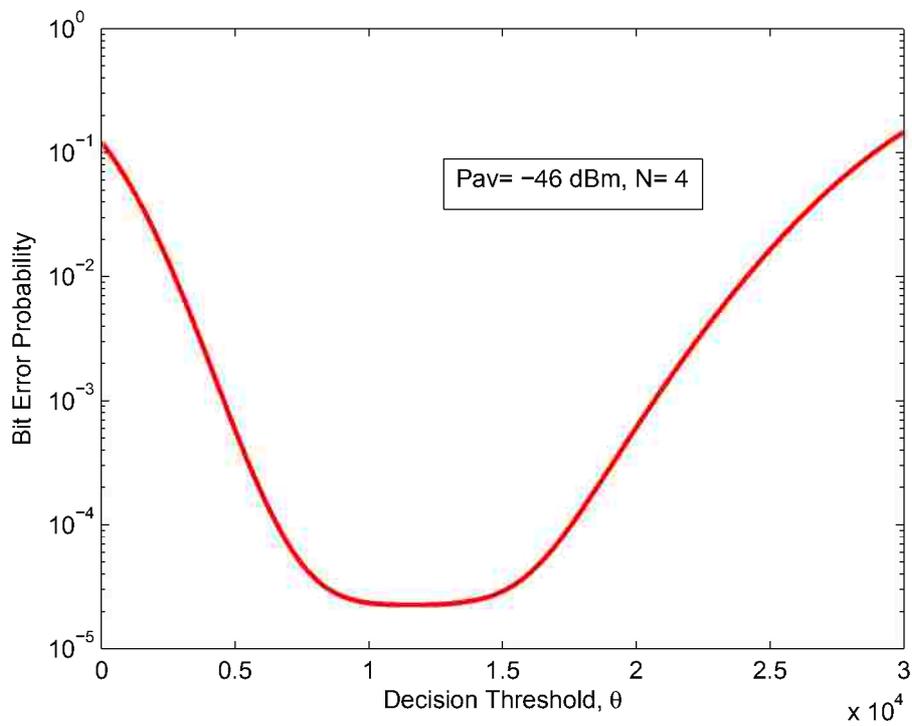FIGURE 5.9 Total Throughput versus average-peak laser power, P_{av}

FIGURE 5.10 Bit error probabilities for chip-level receiver versus the decision threshold θ for Protocol 1.